ORIGINAL ARTICLE

Proteomic analysis of the human hippocampus identifies neuronal pentraxin 1 (NPTX1) as synapto-axonal target in late-stage Parkinson's disease

Carmina C. Warth Perez Arias[1,2,3] | Ivan Silbern[3,4,5] | Lucas Caldi Gomes[1,2,6] | Hannes Wartmann[7] | Vivian Dambeck[1,2] | Jonas Fanz[8,9] | Lisa Neuenroth[5] | Mathias Bähr[1,10] | Tiago F. Outeiro[2,11,12,13,14] | Stefan Bonn[3,4,15] | Christine Stadelmann-Nessler[8] | Silvio O. Rizzoli[2,3,10,16] | Christof Lenz[3,4,5] | Henning Urlaub[3,4,10,17] | Paul Lingor[1,3,6,18,19]

[1]Department of Neurology, University Medical Center Göttingen, Göttingen, Germany

[2]Center for Biostructural Imaging of Neurodegeneration, Göttingen, Germany

[3]Collaborative Research Center 1286 "Quantitative Synaptology", University of Göttingen, Göttingen, Germany

[4]Bioanalytical Mass Spectrometry Group, Max Planck Institute for Multidisciplinary Sciences, Göttingen, Germany

[5]Bioanalytics Group, Department of Clinical Chemistry, University Medical Center Göttingen, Göttingen, Germany

[6]Clinical Department of Neurology, School of Medicine, rechts der Isar Hospital, Technical University of Munich, Munich, Germany

[7]Institute for Medical Systems Biology, University Medical Center Hamburg-Eppendorf, Hamburg, Germany

[8]Department of Neuropathology, University Medical Center Göttingen, Göttingen, Germany

[9]Göttingen Campus Institute for Dynamics of Biological Networks (CIDBN), University of Göttingen, Göttingen, Germany

[10]Cluster of Excellence "Multiscale Bioimaging: from Molecular Machines to Networks of Excitable Cells" (MBExC), University of Göttingen, Göttingen, Germany

[11]Max Planck Institute for Natural Sciences, Göttingen, Germany

[12]Faculty of Medical Sciences, Translational and Clinical Research Institute, Newcastle University, UK

[13]Scientific employee with an honorary contract at German Center for Neurodegenerative Diseases (DZNE), Göttingen, Germany

[14]Department of Experimental Neurodegeneration, University Medical Center Göttingen, Göttingen, Germany

[15]Center for Biomedical AI, University Medical Center Hamburg-Eppendorf, Hamburg, Germany

[16]Department for Neuro- and Sensory Physiology, University Medical Center Göttingen, Göttingen, Germany

[17]Department of Clinical Chemistry, University Medical Center Göttingen, Göttingen, Germany

[18]German Center for Neurodegenerative Diseases (DZNE), Munich, Germany

[19]Munich Cluster for Systems Neurology (SyNergy), Munich, Germany

Correspondence
Paul Lingor, Clinical Department of Neurology, School of Medicine, rechts der Isar Hospital, Technical University of Munich, Ismaninger Strasse 22, 81675 Munich, Germany.
Email: paul.lingor@tum.de

Abstract

Parkinson's disease (PD) affects a significant proportion of the population over the age of 60 years, and its prevalence is increasing. While symptomatic treatment is available for motor symptoms of PD, non-motor complications such as dementia result in diminished life quality for patients and are far more difficult to treat. In this study,

we analyzed PD-associated alterations in the hippocampus of PD patients, since this brain region is strongly affected by PD dementia. We focused on synapses, analyzing the proteome of post-mortal hippocampal tissue from 16 PD cases and 14 control subjects by mass spectrometry. Whole tissue lysates and synaptosomal fractions were analyzed in parallel. Differential analysis combined with bioinformatic network analyses identified neuronal pentraxin 1 (NPTX1) to be significantly dysregulated in PD and interacting with proteins of the synaptic compartment. Modulation of NPTX1 protein levels in primary hippocampal neuron cultures validated its role in synapse morphology. Our analysis suggests that NPTX1 contributes to synaptic pathology in late-stage PD and represents a putative target for novel therapeutic strategies.

KEYWORDS
neurodegeneration, Parkinson's disease, proteomics, synaptic dysfunction

1 | INTRODUCTION

Parkinson's disease (PD) is characterized by a progressive degeneration in multiple regions of the central nervous system giving rise to a broad range of motor and non-motor symptoms. The prominent loss of midbrain dopaminergic neurons causes the characteristic extrapyramidal symptoms in PD (Dickson et al., 2009). Dopamine imbalance affects synaptic transmission, synaptic vesicle exocytosis, and vesicle cycling (Chung et al., 2009; Lee et al., 2010; Matta et al., 2012), with evidence supporting early synaptic dysfunction and synaptic loss preceding the loss of neuronal somata (Cheng et al., 2010; Schirinzi et al., 2016).

In addition to motor impairment, dementia is a key manifestation of advanced PD, affecting up to 80% of patients in later disease stages, resulting in a six-times higher prevalence than in age-matched subjects (Aarsland et al., 2003). PD dementia has been linked to hippocampal atrophy, with hippocampal volume reduction being correlated to memory impairment (Camicioli et al., 2003; Riekkinen et al., 1998). The current study focused on the proteomic correlate of late-stage PD, addressing alterations in the hippocampus of post-mortem tissue with a special focus on synapto-axonal dysfunction. Our results describe PD-related alterations in the hippocampal proteome and identify NPTX1 as a novel target protein for disease-modifying treatment approaches.

2 | METHODS

2.1 | Human post-mortem hippocampal samples

Frozen human hippocampal samples were obtained from the Parkinson's UK Brain Bank (Imperial College London, London, UK). Samples from 16 PD patients and 14 respective age-correlated control subjects (CTR) were analyzed. Informed consent of donors was incurred by the brain bank sample provision. Table S1 summarizes clinical information about the subjects. Punch biopsies were taken for whole tissue lysates (WTL) as previously described in Caldi

Gomes et al. (2022) with few adaptations (detailed in the Supporting Information methods section). For synaptosomal fractions (SF), samples from six PD patients and four CTR were used. The mass spectrometry analyses described here were not preregistered.

2.2 | Differential expression analysis of whole tissue lysate samples by data-independent acquisition mass spectrometry (DIA-MS)

WTL samples were subjected to DIA-MS as described in Caldi Gomes et al. (2022) with few adaptations. More details about the experimental setup for DIA-MS runs are described in the Supporting Information methods. After DIA-MS runs, normalized protein abundance counts for each patient were log transformed. The limma R package (RRID:SCR_010943) was used for differential expression (DE) analysis followed by Benjamini–Hochberg correction for multiple testing. Proteins with an adjusted p-value <0.05 were considered statistically differentially expressed. For a detailed description, refer to Supporting Information methods.

2.3 | Differential expression analysis of synaptosomal fractions by tandem mass tag-mass spectrometry analysis

2.3.1 | Synaptosomal fraction isolation and preparation for LC–MS/MS analysis

To isolate the SF from post-mortem hippocampus, snap-frozen tissue blocks, 600 mg each, were submerged into 5 mL of a cold homogenization buffer (320 mM sucrose and 5 mM HEPES in water) and homogenized using a Teflon/glass homogenizer. Crude synaptosomal pellet was obtained by a two-step centrifugation in a SS 34 fixed angle rotor (Thermo Fisher Scientific) for 2 min at 2988 g and for 12 min at 14462 g, respectively. Crude synaptosomes were resuspended in the homogenization buffer and further purified by differential centrifugation

using discontinuous Ficoll gradient (6%/9%/13%, wt/v Ficoll in the homogenization buffer). The gradients were centrifuged for 35 min at 86 575 g in an SW 41 swinging bucket rotor (Beckman Coulter). Two synaptosomal bands at the interfaces between 6%/9% and 9%/13% Ficoll were collected, pooled, and washed with the homogenization buffer. Pelleted synaptosomes were lysed in 50 μL of lysis buffer (4% SDS, 100 mM HEPES, 1 mM EDTA, 1×Halt Protease and phosphatase inhibitor cocktail in water) and sonicated for 10 min using 30 s on/30 s off—cycles at the maximum output of Bioruptor ultrasonication device (Diagenode). Protein concentration was determined using BCA protein assay according to the manufacturer's instructions. Two hundred micrograms of proteins per sample were reduced and alkylated following the incubation with 10 mM TCEP and 40 mM CAA for 30 min at 37°C. For protein purification steps, refer to the protocol by Hughes et al. (2019) Purified proteins were digested overnight at 37°C using trypsin (1:20 trypsin-to-protein ratio, wt/wt) in digestion buffer (10% (v/v) trifluoroethanol (TFE), 100 mM TEAB in water). Ten individual samples (6×PD and 4×CTR) and one technical replicate (separate synaptosomal preparation of a PD sample) were labeled using TMT11 labeling reagents according to the manufacturer's instructions. The labeling reaction was quenched with 1% (v/v) of hydroxylamine in water. Samples were pooled, cleaned using the pre-packed C18 spin columns (Harvard Apparatus), and concentrated in a Savant SpeedVac vacuum concentrator (SpeedVac, Thermo Fisher Scientific). TMT11-labeled peptides were pre-fractionated using reversed-phase chromatography under basic pH (bRP, buffer A: 10 mM NH4OH in water, pH ~10; buffer B: 10 mM NH4OH and 80% (v/v) ACN in water, pH ~10), as an adaptation to the protocol described by Silbern and colleagues (Silbern et al., 2021). Specific details about bRP equipment are also described in Silbern et al. (2021). The bRP-column was equilibrated with 95% buffer A and 5% buffer B mixture. A linear gradient ranging from 5% to 50% buffer B for 74 min followed by a washing step at 90% buffer B for 5 min was applied. One-minute fractions were collected and concatenated into 24 final fractions, as suggested by Wang and colleagues (Wang et al., 2011). BRP-Fractions were subsequentially snap-frozen in liquid nitrogen and dried in the SpeedVac.

2.3.2 | DDA-MS of synaptosomal fractions

Dried peptides were re-dissolved in 2% (v/v) ACN 0.1% (v/v) TFA in water and injected as a technical duplicate onto a C18 PepMap100-trapping column (0.3×5 mm, 5 μm, Thermo Fisher Scientific) connected to an in-house packed C18 analytical column (75 μm×300 mm; Reprosil-Pur 120 C18 AQ, 1.9 μm, Dr. Maisch GmbH). The columns were pre-equilibrated using a mixture of 98% buffer A (0.1% (v/v) FA in water), 2% buffer B (80% (v/v) ACN, and 0.1% (v/v) FA in water). Liquid chromatography was controlled by UltiMate 3000 RSLC Nanosystem (Thermo Fisher Scientific). Peptides were eluted using a 120 min-linear gradient ranging from 2% to 7% buffer B over 1 min and 7% to 45% buffer B over 105 min, followed by a washing step at 90% of buffer B for 5 min. Eluting peptides were sprayed into an Orbitrap Fusion Lumos Tribrid mass spectrometer (Thermo Fisher Scientific). MS1 scans (350–2000 m/z)

were acquired in a positive ion mode with a resolution of 120000 at 200 m/z, 5e5 automatic gain control (AGC) target, and 50 ms maximum injection time. Precursor ions (allowed charges 2–7, dynamic exclusion 40 s) were isolated using a 1.6 m/z isolation window and fragmented at normalized collision energy (NCE) of 38%. The MS2 fragment spectra were acquired with a resolution of 15000, 2.5e5 AGC target, and 40 ms maximum injection time. The ten most intense fragment ions were selected for a subsequent SPS-MS3 scan using an isolation window of 2 m/z and NCE of 45%. The SPS-MS3 spectra were acquired at a resolution of 60000 and maximum injection time of 118 ms.

2.3.3 | Data analysis of synaptosomal fraction data

Raw files were processed using MaxQuant version 1.6.10.2. (Cox et al., 2011; Tyanova et al., 2016) (RRID:SCR_014485). Cysteine carbamidomethylation was selected as a fixed modification, while methionine oxidation and acetylation of protein N-termini were allowed as variable modifications. Specific tryptic peptides with up to two missed cleavage sites and 5 variable modifications in total were allowed. Quantification using reporter ions in MS3 (TMT11plex) was selected. MS1 and MS2 mass tolerances were kept at 4.5 and 20 ppm, respectively. Canonical amino acid sequences were retrieved from Uniprot (April 2018) (RRID:SCR_002380). The following steps were conducted in R statistical programming language using custom scripts available upon request. In brief, potential contaminants and matches to reverse sequences reported by MaxQuant were filtered out. Protein groups with less than two razor or unique peptides identified and protein groups containing four or more missing quantitative values were excluded from the analysis. Missing values were imputed for each TMT channel individually by random sampling from a gauss distribution with a mean at the 10% quantile and a half standard deviation of the log-transformed intensities. More details about DDA-MS runs for SF are described in the statistics section and the Supporting Information methods.

2.4 | Western blot analysis

Post-mortem hippocampal lysate membranes were incubated with primary antibodies (NPTX1: 1:100, Becton Dickinson, RRID:AB_397755; SYN1: 1:1.000, Synaptic Systems, RRID:AB_11042000 and/or GAPDH: 1:1.000, HyTest, and RRID:AB_1616722) and secondary antibodies (goat-anti-rabbit-HRP, RRID:AB_2099233, and horse-anti-mouse-HRP, 1:10.000, RRID:AB_330924 Cell Signaling) to determine protein quantities. More details about the experimental setup described in the Supporting Information methods.

2.5 | Weighted correlation network analysis (WGCNA) of whole tissue lysate samples

Pairwise correlations of protein expression patterns of all identified proteins from WTL were calculated, in order to reduce the

large data set into manageable modules of co-expressed proteins. The reduced data set was in turn used to characterize biological relevance of potential modules of interest. The calculation of the weighted co-expression network was conducted using the freely accessible R package WGCNA (RRID:SCR_003302), following the available tutorial (Langfelder & Horvath, 2008). Network construction and module detection option were used for module construction (thresholding power of 4 and minModuleSize of 25), keeping all default settings.

2.6 | Weighted correlation network analysis (WGCNA) of synaptosomal fraction samples

Similar to what was done for the WTL results, modules were constructed for the data set of identified proteins from the SF, with a thresholding power of 10 and minModuleSize of 80 to account for the same number of modules (10)—as established previously with WTL samples to enable comparisons.

2.7 | Gene Ontology (GO) and functional annotation

Functional annotation analysis and protein–protein interaction networks were created using STRING Platform v.11.0b (Szklarczyk et al., 2019). Significance for enriched terms was considered at FDR < 0.05. For the functional annotation analysis of WGCNA-generated modules, the WEB-based Gene SeT AnaLysis Toolkit (Liao et al., 2019; RRID:SCR_006786) was employed under standard settings (reference gene set list: genome–protein-coding), making use of the redundancy reducing affinity propagation method for post-processing.

2.8 | Immunohistochemistry for human hippocampal samples

Paraffin-embedded hippocampal tissue sections of one PD and one CTR were deparaffinized and pre-treated according to previously published protocols (Fard et al., 2017). Primary NPTX1 antibody (1:100, Becton Dickinson, RRID:AB_397755) was incubated overnight at room temperature followed by visualization with the HRP-based EnVision Kit (RRID:AB_2890017; Dako).

2.9 | Primary hippocampal neuron cultures, recombinant NPTX1 treatment, immunocytochemistry, and synapse morphology assessment

Animals used for primary cell culture preparation were provided by the Central Animal Facility (ZTE) of the University Medical Center Göttingen, Göttingen, Germany. All animal experiments followed the regulations of the local animal research council (LAVES, Niedersächsisches Landesamt für Verbraucherschutz und Lebensmittelsicherheit, Reg. nr. G13/1332) and legislation of the State of Lower Saxony, Germany. Previous to the preparation, pregnant female animals were kept in standard multiple housing (maximum four animals per cage) under environmentally controlled conditions (temperature, humidity, 12-h dark/light cycle) and fed ad libitum. No randomization was performed to allocate animals in the study. Pregnant females (C57BL6/J mice) were fully anesthetized in a CO_2 chamber to avoid drug residues in the offspring. After spinal reflexes were tested (by pinching of the tail, upper and lower limbs with a laboratory tweezer), animals were subsequently euthanized by cervical dislocation. Primary hippocampal neurons were prepared from mouse pups at postnatal day 0 (P0). Fourteen primary cultures were employed, accounting to 14 dams and around 112 pups used for all preparations/experimental replicates. Recombinant NPTX1 (0.23 μg, R&D Systems, cat. no. 7707-NP-050) was added daily for 7 days. After fixation with 4% paraformaldehyde, ICC was performed with primary (NPTX1: 1:50, Becton Dickinson, RRID:AB_397755; SYN1: 1:500, Synaptic Systems, RRID:AB_11042000) and conjugated secondary antibodies (AlexaFluor AffiniPure fluorescent dye, 1:250, anti-rabbit, Jackson ImmunoResearch, AB_2337913, or Cy3 AffiniPure fluorescent dye, 1:250, anti-mouse, Jackson ImmunoResearch, AB_2338447) were used. Extended description of ICC experiments is placed in the Supporting Information methods. For image analysis, custom-written Matlab (RRID:SCR_001622) scripts were used to measure and determine synapse morphology (details in Supporting Information methods).

2.10 | Statistics

Demographic differences between the analyzed groups of patients were considered significantly different with $p < 0.05$ according to Fisher's exact test or two-sample t-test with equal variance assumed. The number of subjects that composed the analyzed human cohort was exclusively dependent on post-mortem sample availability by the selected Brain Bank. For the animal experiments, all available mouse pups were used from each litter for the primary cell culture preparations and no sample size calculation for the number of pups used was performed. Three to five experimental replicates were used for each cell culture experiment. For proteomics analyses, peak areas were extracted using information from the MS/MS library at an FDR of 1% (Lambert et al., 2013). Normalized protein abundance counts for each patient were log transformed before differential expression analyses were performed. Benjamini-Hochberg correction was used to adjust p-values for multiple testing. Log2-transformed reporter ion intensities were then normalized using Tukey median polishing and subjected to statistical testing using limma package by Smyth (Smyth et al., 2005) (RRID:SCR_010943). Differences in protein group intensities between PD- and control samples were expressed as log2 fold changes (PD/Control). Protein groups showing Empirical-Bayes

moderated *p*-values <0.05 were considered differentially expressed and were subjected for bioinformatic analyses. Complete statistical reports for proteomics results are presented in Tables S2 and S3. Two-sided *t*-tests were employed for the statistical analyses of quantified western blotting band intensities. qRT-PCR datasets were analyzed using Mann–Whitney U tests for non-normal data.

3 | RESULTS

Protein changes were quantified in the post-mortal hippocampus of patients with PD (*n* = 16) and corresponding age-correlated control subjects (CTR) (*n* = 14). The groups showed no significant difference in demographic and clinical data (Table S1). Two separate sample preparations, whole tissue lysates (WTL) and synaptosomal fractions (SF), were analyzed (Figure 1a).

3.1 | Proteomic analysis, differential expression, and functional annotation

Proteomic analysis was conducted via DIA-MS/DDA-MS (for WTL and SF respectively). MS experiments quantified a total of 2089 protein groups for the WTL and 2413 protein groups for the SF. Differential expression analysis of the WTL found 55 significantly differentially expressed (DE) proteins between PD and CTR (Figure 1b–d), while analysis of SF yielded 194 DE proteins (Figure 1e–g).

Protein–protein interaction (PPI) networks of the DE proteins of the WTL showed prominent clusters composed, among others, of proteins involved in axonal growth such as BASP1, GAP43, and AGRN, as well as signal transduction mediators such as YWHAH, YWHAQ, and YWHAE (Figure S1), with YWHAE being also present in the SF, clustering among others with NPTXR (Figure S1). A functional annotation analysis yielded top enriched Gene Ontology (GO) terms involved in *(vesicle-mediated) transport* and *(membrane) localization* (Figure S1) suggestive of a marked dysregulation of processes involved in synapto-axonal function.

3.2 | Network analysis of co-expressed protein expression patterns and biological relevance

Characteristic protein expression levels across all patients were evaluated using WGCNA (Langfelder & Horvath, 2008), dividing each data set into modules based on similar expression patterns of protein levels. In the WTL samples, 10 modules were identified (Figure 2a), and the SF data were adapted to yield the same number of modules for comparability (Figure 2d). In a functional annotation analysis, umbrella terms were used to combine related GO terms that were significantly enriched in the individual WGCNA modules (all enriched terms shown in Table S5). Analysis revealed GO terms widespread across several modules of both sample preparations such as *metabolic process*, *cellular localization*, and *transport*, as well as terms specific to distinct modules (Figure S2). Among all modules, module 03 of the WTL data (W03) showed a strong synaptic profile, with the functional annotation analysis revealing biological processes strongly related to *synapse* and *synaptic vesicles*. Among the 184 proteins found in this module, 14 proteins were previously found to be differentially expressed in the DE analysis, including BASP1, GAP43, PEA15, SYN1, and NPTX1 (Figure 2b,c). Interestingly, module 01 (S01) of the SF showed an almost exact overlap in top-ranked enriched GO terms. Out of the 495 proteins in the S01 module, 23 proteins were DE proteins, including DBN1, CAMK2A, and NPTXR (Figure 2e,f). The integration of the analyzed data sets enabled a focused selection of proteins of interest involved in synaptic dysfunction in the hippocampus of PD. Because NPTX1 and its receptor NPTXR were identified as differentially expressed and enriched in the synapto-axonal WGCNA modules, and since NPTX1 has been associated with synaptic dysfunction in neurodegenerative diseases previously (Coutelier et al., 2021; Deppe et al., 2022; Figueiro-Silva et al., 2015; Ma et al., 2018), and even proposed as an early biomarker for Alzheimer's disease (AD; Duits et al., 2018), we focused the further analysis on NPTX1 as a particularly promising target.

3.3 | Expression of NPTX1 in human brain tissue

To assess the expression of NPTX1 in human brain tissue, we performed immunohistochemistry on paraffin-embedded hippocampal tissue sections and found a maximum synaptic expression in the CA4 region (Figure 3a–d). Western blot analyses confirmed the increased abundance of NPTX1 in PD brains (Figure 3e,f).

3.4 | Modulation of NPTX1 in primary hippocampal cell cultures

To mimic the increased levels of NPTX1 observed in PD samples, recombinant NPTX1 protein was added to primary P0 mouse

FIGURE 1 Overview of proteomic analysis. (a) Scheme of workflow from sample acquisition via needle biopsy/synaptosomal fractionation to MS analyses and data treatment. (b, e) Volcano scatter plots showing differential expression of proteins between PD and CTR from proteins identified from whole tissue lysates and synaptosomal fractions. *p*-values (−log10) are plotted against fold changes (log2). Dotted line at *p*-value 0.05. Cool colors (blue-yellow) show proteins down-regulated in PD, and warm colors (orange-red) show proteins upregulated in PD. Circle radius represents fold change. Differential expression analysis was performed with the *limma* package (Smyth et al., 2005) in R. (c, f) Overview of consistently quantified proteins from whole tissue lysate samples and synaptosomal fractions, as well as consistently quantified proteins with differential expression. Red arrows show up-regulation; blue arrows show down-regulation. (d, g) Heatmaps of the top 55 and 50 differentially expressed proteins from whole tissue lysate samples and synaptosomal fractions respectively. Z score calculated from normalized counts for each patient.
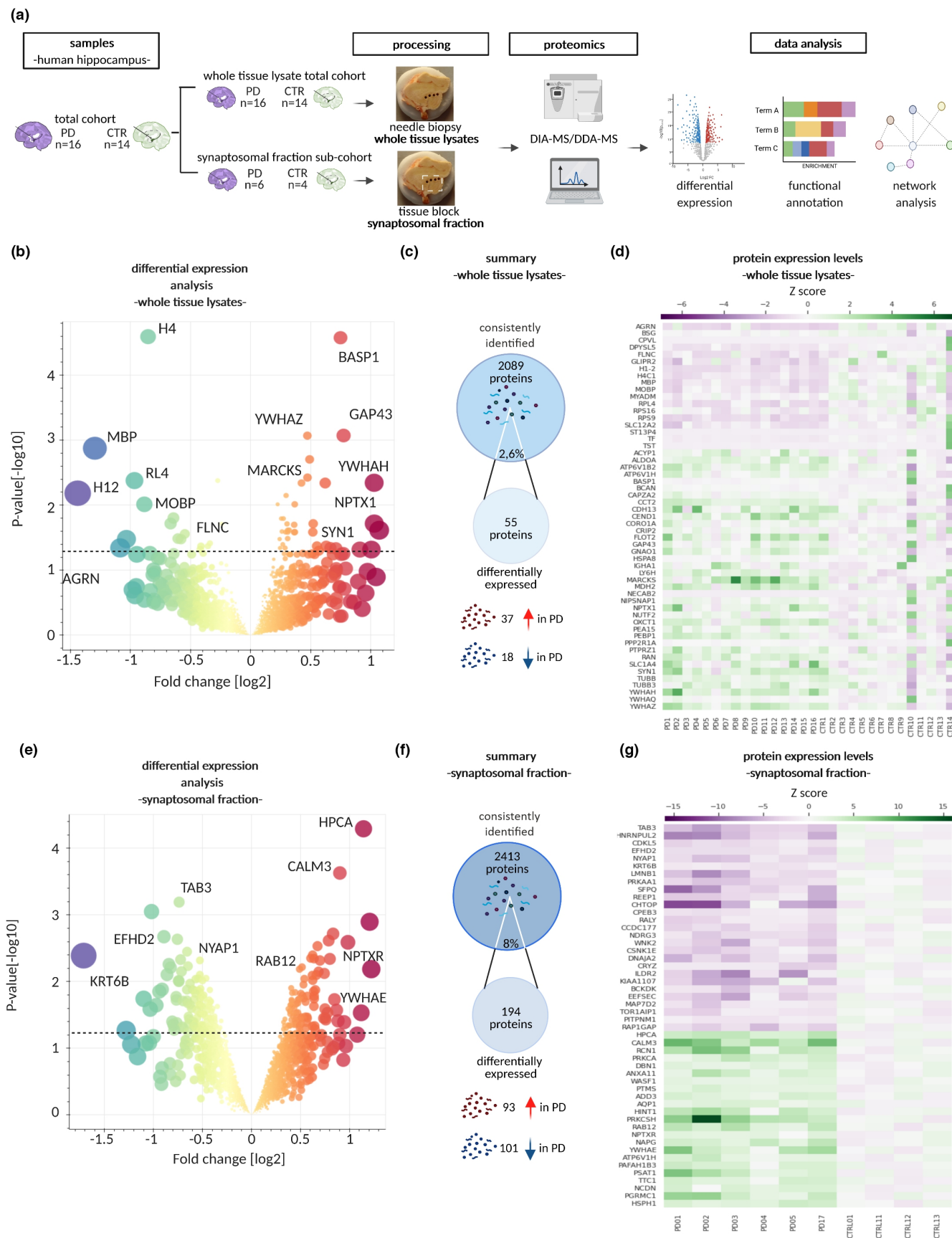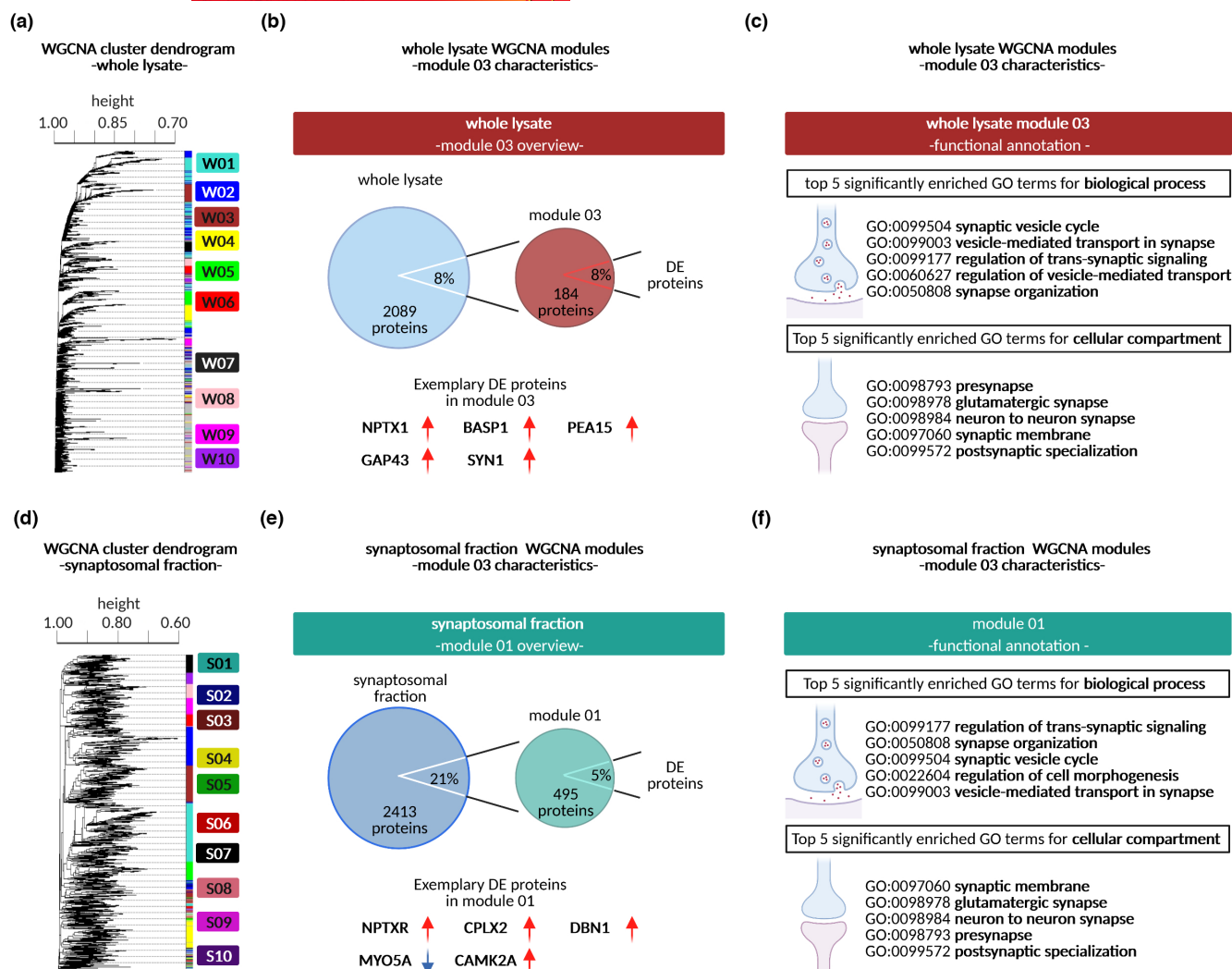
FIGURE 2 Co-expression network construction and functional annotation analysis. Cluster dendrogram with individual proteins from whole tissue lysates (a) and synaptosomal fractions (d) depicted in rows accompanied by the module assignment. Overview of proteins grouped in synaptic modules from whole tissue lysates (b) and synaptosomal fractions (e), as well as proteins with differential expression found in the modules. Red arrows show up-regulation; blue arrows show down-regulation. Top five GO-*biological processes* terms as well as top 5 GO-*cellular compartment* terms significantly enriched, with an FDR <0.05, are shown for proteins from the synaptic module 03 from whole tissue lysates (c) and synaptic module 01 from synaptosomal fractions (f). Functional annotation analysis was conducted with the "WEB-based Gene SeT AnaLysis Toolkit" (Liao et al., 2019) under standard settings.

hippocampal neuron cultures (Figure 3g). The fixed cell cultures were co-immunostained for NPTX1 and SYN1 to quantify the effects of NPTX1 application on synapse morphology (Figure 3h). Photomicrographs of immunocytochemical stainings were taken, fitting ellipses to ~10 300 individual synapses and quantifying structural characteristics such as synaptic area and major and minor axis of the fitted ellipses using a semi-automatic algorithm (Figure 3i). We found a significant decrease in the area of NPTX1-treated synapses compared with vehicle-treated cultures (37.7 vs. 39.73 a.u. respectively, $p = 0.01$). Furthermore, while the major axis was unchanged, the minor axis showed a significant increase in treated cells (5.34 vs. 5.32 a.u, respectively, $p = 2.52 \times 10^{-5}$), while also presenting a significant increase in mean intensity per synapse in NPTX1-treated neurons (16.16 vs. 15.19 a.u., respectively, $p < 2.2 \times 10^{-16}$; Figure 3j).

4 | DISCUSSION

In the work presented here, we addressed the proteomic composition of hippocampal tissue, including SF, from post-mortem samples of patients with PD and identified NPTX1 as promising target protein contributing to synaptic pathology in PD.

Our initial analysis identified 2089 unique proteins from the WTL sample and 2413 unique proteins from the SF samples, which is in line with previous proteomic studies of human post-mortem tissue of PD patients and for other neurodegenerative diseases. Compared with studies that analyzed Substantia nigra (SN) tissue, revealing 1795 unique detected proteins (Licker et al., 2014), or the analysis of frontal cortex material with 1864 uniquely identified proteins (Shi et al., 2008), our higher detection might be attributable

to both, a high number of available samples ($n = 16$ PD and $n = 14$ CTR) and the high quantification accuracy and precision of DIA-MS. Other studies report a higher number of identified proteins in brain tissue (McKetney et al., 2019; Ping et al., 2018). Nevertheless, studies that employed similar methodological settings also reported similar numbers of consistently quantified proteins (in the range of 2.600–3.300 uniquely identified proteins for WTL of brain samples (Johnson et al., 2020; Seyfried et al., 2017), and in the range of 2.500–3.600 consistently quantified proteins for TMT-labeling mass spectrometry for human biofluids (Higginbotham et al., 2020; Muraoka et al., 2020)). While 55 DE proteins were identified in the WTL cohort, the SF analysis—which included only a smaller subset of WTL samples—did not yield DE proteins after multiple testing correction according to Benjamini–Hochberg. Therefore, a less stringent approach considering empirical Bayes moderated p-values was employed yielding 194 DE proteins. Among the identified DE proteins, we detected several proteins previously addressed in relation to PD, including an increase in several isoforms of the 14–3-3 protein family such as YWHAE, YWHAH, and YWHAQ (Table S2). YWHAE had been previously found in Lewy bodies in the SN of PD patients (Berg et al., 2003) while YWHAH was found to influence the kinetics and products of α-syn aggregation in vitro (Plotegher et al., 2014). Both YWHAH and YWHAE were also found to be upregulated in the synaptosome samples (Table S3). Furthermore, mediators of regenerative axonal growth, BASP1 and GAP43, (Table S2), were among the higher abundant proteins in PD patients. Studies of the nigrostriatal system in PD have shown a decrease in GAP43 mRNA in dopaminergic neurons and a reduction in GAP43 in the neuropil of the SNpc, suggesting a lower regenerative capacity of the dopaminergic system (Saal et al., 2017). Considering the spatial progression proposed by Braak (Braak et al., 2003), where the hippocampus is affected subsequent to the midbrain, the elevated expression of GAP43 and BASP1 in the hippocampus of PD patients might reflect a compensatory mechanism in response to degeneration in other regions.

In addition to the assessment of individual DE proteins, we identified several functional modules by co-expression analysis (Langfelder & Horvath, 2008). Functional annotation revealed modules W03 of the WTL and S01 of the SF data set to be strongly representative of *synapse-related biological processes* as well as *synapse* for top enriched cellular compartments (Figure 2c,f), suggesting these modules as of special interest for the study of synaptic dysfunction in PD. These modules encompassed several DE proteins such as BASP1, GAP43, SYN1, NPTX1, and NPTXR (Figure 2b,e). In addition to the previously addressed involvement of BASP1 and GAP43 in axonal regeneration, NPTX1 had been previously linked to neurodegeneration as a potential plasma biomarker of synaptic dysfunction. NPTX1 belongs to the family of long neuronal pentraxins that are associated with the synaptic scaffolding complex. Both, NPTX1 and its receptor, NPTXR, are mainly expressed by excitatory neurons, and have been shown to play a role in synaptogenesis, and synaptic remodeling, as well as to modulate mitochondrial transport/dynamics, and also the function of AMPA receptors in synapses

(Cho et al., 2008; Clayton et al., 2012; Goodman et al., 1996; Sia et al., 2007; Xu et al., 2003). The expression of NPTX1 is specific to central nervous system tissue, being well characterized in the hippocampus, as well as in the cortex, amygdala, and cerebellum (Schlimgen et al., 1995; Uhlén et al., 2015). NPTX1 has been linked to neurodegeneration by its contribution to activity-dependent apoptosis in neurons (DeGregorio-Rocasolano et al., 2001). Low neuronal activity in mature neurons has been found to induce the expression of NPTX1, modulating mitochondrial dynamics, and reducing synaptic density (Abad et al., 2006; Figueiro-Silva et al., 2015). Models of neurodegeneration in vitro reported increased levels of NPTX1 in dystrophic neurites, as well as NPTX1-induced impairments in synaptic transmission (Abad et al., 2006; Cummings et al., 2017). Interestingly, deregulated expression of neuronal pentraxins (i.e., NPTX1 and NPTX2), as well as NPTXR, has been recently reported in a variety of neurological disorders, including AD, autosomal dominant cerebellar ataxia (ADCA) and frontotemporal dementia (FTD). (Coutelier et al., 2021; Deppe et al., 2022; Duits et al., 2018; Esteve et al., 2021; Figueiro-Silva et al., 2015; Ma et al., 2018). Recent studies also explored the biomarker potential of neuronal pentraxins and their receptors for neurodegenerative diseases (Duits et al., 2018; Dulewicz et al., 2021; Lim et al., 2019, 2020; van der Ende et al., 2019, 2020). In a study addressing excitatory synaptic pathology in mild cognitive impairment (MCI) and AD, NPTX1 levels in plasma were significantly increased in MCI ($n = 33$ MCI, $n = 31$ CTR) (Ma et al., 2018). Additionally, NPTX1 was found to negatively regulate synapse density and excitatory synapse numbers, by modulating neuronal excitability while restricting excitatory synaptic plasticity (Figueiro-Silva et al., 2015). Despite its role in synaptic dysfunction, neuronal pentraxins have not been extensively explored the context of PD to date. Only few studies explored the relevance of neuronal pentraxins for PD pathology (Li et al., 2019; Moran et al., 2008). A couple of studies have recently reported decreased levels of NPTX1, NPTX2, and NPTXR in PD CSF (Lerche et al., 2021; Nilsson et al., 2023).

The early contribution of synaptic dysfunction in the development of PD is well documented (Bellucci et al., 2012; Compta & Revesz, 2021; Schirinzi et al., 2016). Since changes in the expression of NPTX1 have been associated with activity-dependent neurodegenerative events (through the deregulation of mitochondrial function in synapses, alterations in synaptic composition, and impaired neuroplasticity), we hypothesize that dysfunctions in NPTX1/ NPTXR expression might be closely related to PD-related alterations, in particular at early stages of the disease. Thus, we aimed to characterize the expression patterns of NPTX1 and NPTXR in the analyzed cohort, as well as to explore the role of deregulated levels of this candidate for synaptic morphology in vitro.

Our data showed increased levels of NPTX1 in the PD hippocampus—as confirmed by western blot and qRT-PCR—suggesting a novel role for NPTX1 in PD-related changes in synaptic morphology and function. Similar to a previous study on NPTX1 in organotypic hippocampal slices (Cummings et al., 2017), we increased extracellular levels of NPTX1 modeling its secretion (Yuzaki, 2018; Figure 3g). Our
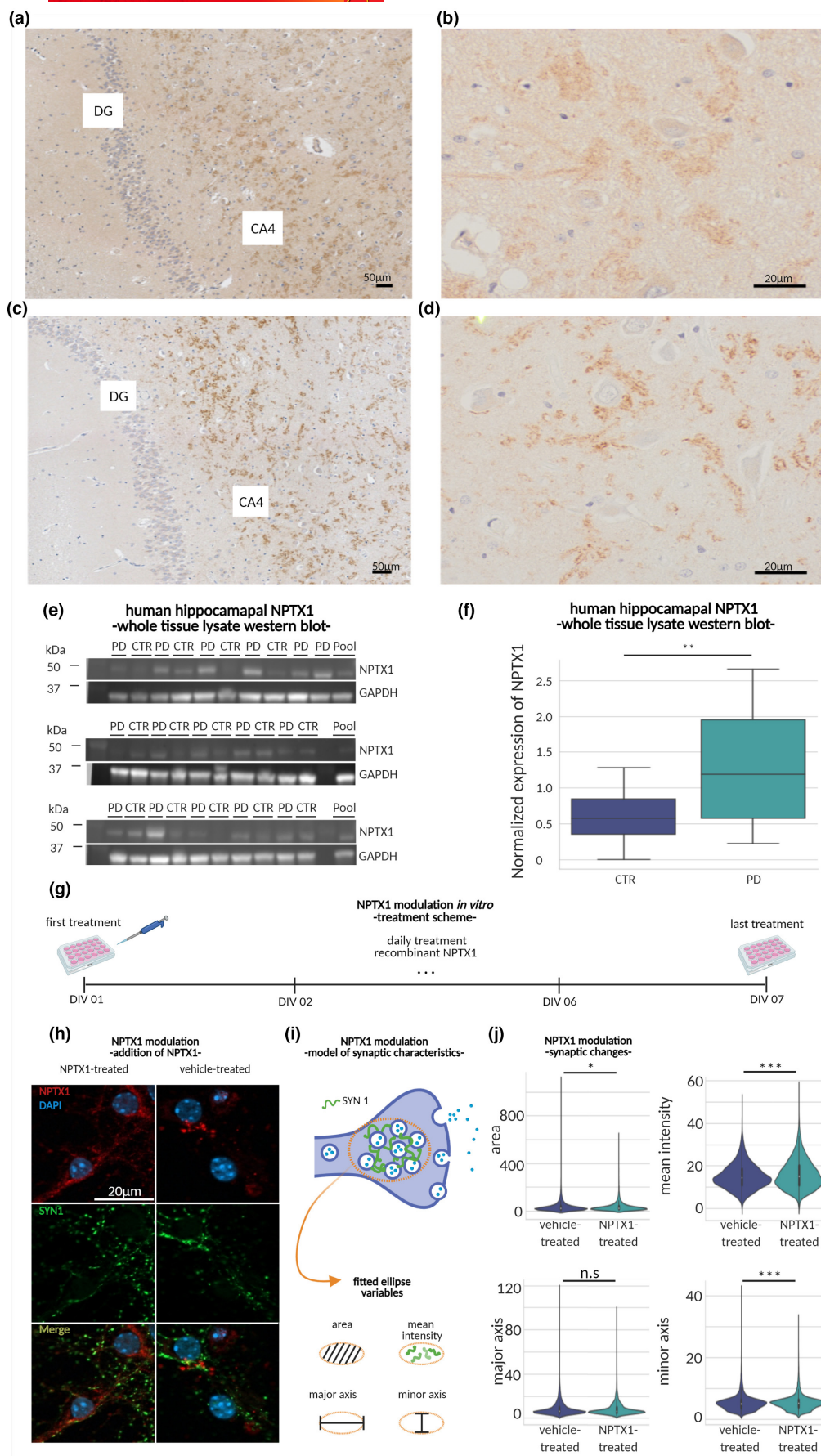
(a)

(b)

(c)

(d)

(e) human hippocamapal NPTX1
-whole tissue lysate western blot-

(f) human hippocamapal NPTX1
-whole tissue lysate western blot-

(g) NPTX1 modulation *in vitro*
-treatment scheme-

(h) NPTX1 modulation
-addition of NPTX1-

(i) NPTX1 modulation
-model of synaptic characteristics-

(j) NPTX1 modulation
-synaptic changes-

FIGURE 3   Human NPTX1 expression and validation experiments in vitro. (a–d) Representative photomicrographs of cytoplasmic NPTX1 expression with maxima in human CA4 hippocampal area. DG: dentate gyrus, CA: Cornu Ammonis. Representative NPTX1 stainings stand for (a) PD sample (100× magnification); (b) Magnified view (400x) of neurons located in CA4 field of (a); (c) control sample (100× magnification); (d) Magnified view (400×) of neurons located in CA4 field of (c). (e) Antibody signals of NPTX1 (50 kDa) and GAPDH in western blots. All available patient samples ($n = 16$ PD, $n = 14$ CTR) were loaded in equal amounts and a pool of all samples was loaded additionally on each gel (pool). (f) Quantification of NPTX1 signal shown in (e). Signal was normalized to housekeeping GAPDH and to the pool signal. Significant increase in NPTX1 signal in PD samples. **p-value $= 0.007$, t-value $= 2.774$, DF $= 54$, two-sided t-test. (g) Scheme of chronic NPTX1 treatment of murine hippocampal cultures. Cells were treated daily, starting at DIV01, for 7 days with recombinant NPTX1. (h) Exemplary immunocytochemical stainings of NPTX1-treated (+NPTX1) and vehicle-treated neurons (+vehicle). Cells were fixated at DIV08 and immunostained for NPTX1 (red) and synapsin 1 (SYN1, green). SYN1 signal was used for synaptic morphology assessment. (i, j) Quantification of synaptic morphology in NPTX1- and vehicle-treated hippocampal neurons via semi-automatically quantified ellipse variables.

study showed a significant alteration of synapse morphology in neurons treated with NPTX1, resulting in significantly smaller and stubbier shapes compared with vehicle-treated neurons (Figure 3j). Allied with the well-characterized contribution of synaptic dysfunction in PD and the evidence from neurophysiological studies showing an effect of presynaptic activity on postsynaptic dendritic spines (Nägerl et al., 2004; Yuste & Bonhoeffer, 2001), our results support the role of synaptic alterations in PD and suggest NPTX1 as a new protein target.

5 | CONCLUSIONS

In summary, we characterized changes in protein expression levels of advanced-stage human hippocampal PD samples, finding an altered expression level in several targets involved in synapto-axonal function. Among the dysregulated proteins, NPTX1 appeared as a promising and novel target protein in the synaptic hippocampal pathology of PD. The increased abundance of NPTX1 captured by proteomics and validated by western blot (Figure 3f) was also confirmed on the gene level (qRT-PCR results; Figure S5), and in vitro modulation of NPTX1 levels confirmed morphological changes in synapses of hippocampal neuron cultures. These findings suggest a new role for NPTX1 in the synaptic pathology of the hippocampus in PD and PD dementia. Our results speak for further investigation of the mechanism of extracellular NPTX1 elevation and suggest further studies analyzing whether inhibition of NPTX1 has beneficial disease-modifying effects in PD.

AUTHOR CONTRIBUTIONS

C.C.W.P.A. designed and performed research/experiments, analyzed and interpreted data, and wrote the paper. I.S. performed proteomics experiments for SF samples, analyzed and interpreted data, and wrote the paper. L.C.G. contributed to the sample acquisition process, performed research/experiments, interpreted data, and wrote and revised the paper. H.W. performed bioinformatics analyses and revised the paper. V.D. performed research/experiments and revised the paper. J.F. performed stainings for human post-mortem tissue and wrote the paper. L.N. performed proteomics experiments and wrote the paper. M.B. contributed with analytic tools/equipment and revised the paper. T.F.O. designed the research and revised the paper. S.B. designed the research, performed bioinformatic analyses, and revised the paper. C.S-N. contributed with analytic tools and equipment, contributed to staining experiments for human post-mortem samples and revised the paper. S.O.R. designed the research and revised the paper. C.L. designed and performed research/proteomics experiments, analyzed and interpreted data, and wrote the paper. H.U. contributed with analytic tools/equipment and revised the paper. P.L. designed the research, obtained samples, contributed with analytic tools/equipment, analyzed and interpreted data, wrote and revised the paper. All authors read and approved the final manuscript.

ACKNOWLEDGMENTS

FUNDING INFORMATION

CONFLICT OF INTEREST STATEMENT

Mathias Bähr is a former editor of the Journal of Neurochemistry. Tiago F. Outeiro is an editor in the Journal of Neurochemistry.

PEER REVIEW

The peer review history for this article is available at https://www.webofscience.com/api/gateway/wos/peer-review/10.1111/jnc.15924.

DATA AVAILABILITY STATEMENT

ORCID

Lucas Caldi Gomes https://orcid.org/0000-0003-4959-2169
Tiago F. Outeiro https://orcid.org/0000-0003-1679-1727
Paul Lingor https://orcid.org/0000-0001-9362-7096

REFERENCES

Aarsland, D., Andersen, K., Larsen, J. P., & Lolk, A. (2003). Prevalence and characteristics of dementia in Parkinson disease: An 8-year prospective study. *Archives of Neurology*, 60(3), 387. https://doi.org/10.1001/archneur.60.3.387

Abad, M. A., Enguita, M., DeGregorio-Rocasolano, N., Ferrer, I., & Trullas, R. (2006). Neuronal pentraxin 1 contributes to the neuronal damage evoked by amyloid- and is overexpressed in dystrophic neurites in Alzheimer's brain. *Journal of Neuroscience*, 26(49), 12735–12747. https://doi.org/10.1523/JNEUROSCI.0575-06.2006

Bellucci, A., Zaltieri, M., Navarria, L., Grigoletto, J., Missale, C., & Spano, P. (2012). From α-synuclein to synaptic dysfunctions: New insights into the pathophysiology of Parkinson's disease. *Brain Research*, 1476, 183–202. https://doi.org/10.1016/j.brainres.2012.04.014

Berg, D., Riess, O., & Bornemann, A. (2003). Specification of 14-3-3 proteins in Lewy bodies. *Annals of Neurology*, 54(1), 135. https://doi.org/10.1002/ana.10621

Braak, H., Del Tredici, K., Rüb, U., A I De Vos, R., Jansen Steur, E. N. H., & Braak, E. (2003). Staging of brain pathology related to sporadic Parkinson's disease. *Neurobiology of Aging*, 24(2), 197–211. https://doi.org/10.1016/S0197-4580(02)00065-9

Caldi Gomes, L., Galhoz, A., Jain, G., Roser, A., Maass, F., Carboni, E., Barski, E., Lenz, C., Lohmann, K., Klein, C., Bähr, M., Fischer, A., Menden, M. P., & Lingor, P. (2022). Multi-omic landscaping of human midbrains identifies disease-relevant molecular targets and pathways in advanced-stage Parkinson's disease. *Clinical and Translational Medicine*, 12(1), e692. https://doi.org/10.1002/ctm2.692

Camicioli, R., Moore, M. M., Kinney, A., Corbridge, E., Glassberg, K., & Kaye, J. A. (2003). Parkinson's disease is associated with hippocampal atrophy. *Movement Disorders*, 18(7), 784–790. https://doi.org/10.1002/mds.10444

Cheng, H.-C., Ulane, C. M., & Burke, R. E. (2010). Clinical progression in Parkinson disease and the neurobiology of axons. *Annals of Neurology*, 67(6), 715–725. https://doi.org/10.1002/ana.21995

Cho, R. W., Park, J. M., Wolff, S. B. E., Xu, D., Hopf, C., Kim, J., Reddy, R. C., Petralia, R. S., Perin, M. S., Linden, D. J., & Worley, P. F. (2008). MGluR1/5-dependent long-term depression requires the regulated ectodomain cleavage of neuronal pentraxin NPR by TACE. *Neuron*, 57(6), 858–871. https://doi.org/10.1016/j.neuron.2008.01.010

Chung, C. Y., Koprich, J. B., Siddiqi, H., & Isacson, O. (2009). Dynamic changes in presynaptic and axonal transport proteins combined with striatal neuroinflammation precede dopaminergic neuronal loss in a rat model of AAV -Synucleinopathy. *Journal of Neuroscience*, 29(11), 3365–3373. https://doi.org/10.1523/JNEUROSCI.5427-08.2009

Clayton, K. B., Podlesniy, P., Figueiro-Silva, J., López-Doménech, G., Benitez, L., Enguita, M., Abad, M. A., Soriano, E., & Trullas, R. (2012). NP1 regulates neuronal activity-dependent accumulation of BAX in mitochondria and mitochondrial dynamics. *The Journal of Neuroscience: The Official Journal of the Society for Neuroscience*, 32(4), 1453–1466. https://doi.org/10.1523/JNEUROSCI.4604-11.2012

Compta, Y., & Revesz, T. (2021). Neuropathological and biomarker findings in Parkinson's disease and Alzheimer's disease: From protein aggregates to synaptic dysfunction. *Journal of Parkinson's Disease*, 11(1), 107–121. https://doi.org/10.3233/JPD-202323

Coutelier, M., Jacoupy, M., Janer, A., Renaud, F., Auger, N., Saripella, G.-V., Ancien, F., Pucci, F., Rooman, M., Gilis, D., Larivière, R., Sgarioto, N., Valter, R., Guillot-Noel, L., Le Ber, I., Sayah, S., Charles, P., Nümann, A., Pauly, M. G., ... Stevanin, G. (2021). NPTX1 mutations trigger endoplasmic reticulum stress and cause autosomal dominant cerebellar ataxia. *Brain: A Journal of Neurology*, awab407, 1519–1534. https://doi.org/10.1093/brain/awab407

Cox, J., Michalski, A., & Mann, M. (2011). Software lock mass by two-dimensional minimization of peptide mass errors. *Journal of the American Society for Mass Spectrometry*, 22(8), 1373–1380. https://doi.org/10.1007/s13361-011-0142-8

Cummings, D. M., Benway, T. A., Ho, H., Tedoldi, A., Fernandes Freitas, M. M., Shahab, L., Murray, C. E., Richard-Loendt, A., Brandner, S., Lashley, T., Salih, D. A., & Edwards, F. A. (2017). Neuronal and peripheral pentraxins modify glutamate release and may interact in blood-brain barrier failure. *Cerebral Cortex (New York, N.Y.: 1991)*, 27(6), 3437–3448. https://doi.org/10.1093/cercor/bhx046

DeGregorio-Rocasolano, N., Gasull, T., & Trullas, R. (2001). Overexpression of neuronal pentraxin 1 is involved in neuronal death evoked by low K+ in cerebellar granule cells. *Journal of Biological Chemistry*, 276(1), 796–803. https://doi.org/10.1074/jbc.M007967200

Deppe, J., Deininger, N., Lingor, P., Haack, T. B., Haslinger, B., & Deschauer, M. (2022). A novel NPTX1 de novo variant in a late-onset ataxia patient. *Movement Disorders: Official Journal of the Movement Disorder Society*, 37, 1319–1321. https://doi.org/10.1002/mds.28985

Dickson, D. W., Braak, H., Duda, J. E., Duyckaerts, C., Gasser, T., Halliday, G. M., Hardy, J., Leverenz, J. B., Del Tredici, K., Wszolek, Z. K., & Litvan, I. (2009). Neuropathological assessment of Parkinson's disease: Refining the diagnostic criteria. *The Lancet Neurology*, 8(12), 1150–1157. https://doi.org/10.1016/S1474-4422(09)70238-8

Duits, F. H., Brinkmalm, G., Teunissen, C. E., Brinkmalm, A., Scheltens, P., Van der Flier, W. M., Zetterberg, H., & Blennow, K. (2018). Synaptic proteins in CSF as potential novel biomarkers for prognosis in prodromal Alzheimer's disease. *Alzheimer's Research & Therapy*, 10(1), 5. https://doi.org/10.1186/s13195-017-0335-x

Dulewicz, M., Kulczyńska-Przybik, A., Słowik, A., Borawska, R., & Mroczko, B. (2021). Neurogranin and neuronal pentraxin receptor as synaptic dysfunction biomarkers in Alzheimer's disease. *Journal of Clinical Medicine*, 10(19), 4575. https://doi.org/10.3390/jcm10194575

Esteve, A. S., Nilsson, J., Swift, I. J., Heller, C., Russell, L. L., Peakman, G., Convery, R. S., van Swieten, J. C., Seelaar, H., Borroni, B., Galimberti, D., Sanchez-Valle, R., Laforce, R., Moreno, F., Synofzik, M., Graff, C., Masellis, M., Tartaglia, M. C., Rowe, J. B., ... GENetic FTD Initiative. (2021). Differential synaptic marker involvement in the different genetic forms of frontotemporal dementia. *Alzheimer's & Dementia*, 17(S5), e054934. https://doi.org/10.1002/alz.054934

Fard, M. K., van der Meer, F., Sánchez, P., Cantuti-Castelvetri, L., Mandad, S., Jäkel, S., Fornasiero, E. F., Schmitt, S., Ehrlich, M., Starost, L., Kuhlmann, T., Sergiou, C., Schultz, V., Wrzos, C., Brück, W., Urlaub, H., Dimou, L., Stadelmann, C., & Simons, M. (2017). BCAS1 expression defines a population of early myelinating oligodendrocytes in multiple sclerosis lesions. *Science Translational Medicine*, 9(419), eaam7816. https://doi.org/10.1126/scitranslmed.aam7816

Figueiro-Silva, J., Gruart, A., Clayton, K. B., Podlesniy, P., Abad, M. A., Gasull, X., Delgado-García, J. M., & Trullas, R. (2015). Neuronal pentraxin 1 negatively regulates excitatory synapse density and synaptic plasticity. *The Journal of Neuroscience: The Official Journal*

of the Society for Neuroscience, 35(14), 5504–5521. https://doi.org/10.1523/JNEUROSCI.2548-14.2015

Goodman, A. R., Cardozo, T., Abagyan, R., Altmeyer, A., Wisniewski, H.-G., & Vilček, J. (1996). Long pentraxins: An emerging group of proteins with diverse functions. *Cytokine & Growth Factor Reviews, 7*(2), 191–202. https://doi.org/10.1016/1359-6101(96)00019-6

Higginbotham, L., Ping, L., Dammer, E. B., Duong, D. M., Zhou, M., Gearing, M., Hurst, C., Glass, J. D., Factor, S. A., Johnson, E. C. B., Hajjar, I., Lah, J. J., Levey, A. I., & Seyfried, N. T. (2020). Integrated proteomics reveals brain-based cerebrospinal fluid biomarkers in asymptomatic and symptomatic Alzheimer's disease. *Science. Advances, 6*(43), eaaz9360. https://doi.org/10.1126/sciadv.aaz9360

Hughes, C. S., Moggridge, S., Müller, T., Sorensen, P. H., Morin, G. B., & Krijgsveld, J. (2019). Single-pot, solid-phase-enhanced sample preparation for proteomics experiments. *Nature Protocols, 14*(1), 68–85. https://doi.org/10.1038/s41596-018-0082-x

Johnson, E. C. B., Dammer, E. B., Duong, D. M., Ping, L., Zhou, M., Yin, L., Higginbotham, L. A., Guajardo, A., White, B., Troncoso, J. C., Thambisetty, M., Montine, T. J., Lee, E. B., Trojanowski, J. Q., Beach, T. G., Reiman, E. M., Haroutunian, V., Wang, M., Schadt, E., … Seyfried, N. T. (2020). Large-scale proteomic analysis of Alzheimer's disease brain and cerebrospinal fluid reveals early changes in energy metabolism associated with microglia and astrocyte activation. *Nature Medicine, 26*(5), 769–780. https://doi.org/10.1038/s41591-020-0815-6

Lambert, J.-P., Ivosev, G., Couzens, A. L., Larsen, B., Taipale, M., Lin, Z.-Y., Zhong, Q., Lindquist, S., Vidal, M., Aebersold, R., Pawson, T., Bonner, R., Tate, S., & Gingras, A.-C. (2013). Mapping differential interactomes by affinity purification coupled with data-independent mass spectrometry acquisition. *Nature Methods, 10*(12), 1239–1245. https://doi.org/10.1038/nmeth.2702

Langfelder, P., & Horvath, S. (2008). WGCNA: An R package for weighted correlation network analysis. *BMC Bioinformatics, 9*(1), 1–13.

Lee, S., Liu, H.-P., Lin, W.-Y., Guo, H., & Lu, B. (2010). LRRK2 kinase regulates synaptic morphology through distinct substrates at the presynaptic and postsynaptic compartments of the drosophila neuromuscular junction. *Journal of Neuroscience, 30*(50), 16959–16969. https://doi.org/10.1523/JNEUROSCI.1807-10.2010

Lerche, S., Sjödin, S., Brinkmalm, A., Blennow, K., Wurster, I., Roeben, B., Zimmermann, M., Hauser, A., Liepelt-Scarfone, I., Waniek, K., Lachmann, I., Gasser, T., Zetterberg, H., & Brockmann, K. (2021). Protein level of neurotransmitter secretion, synaptic plasticity, and autophagy in PD and DLB. *Movement Disorders, 36*(11), 2595–2604. https://doi.org/10.1002/mds.28704

Li, J., Sun, Y., & Chen, J. (2019). Transcriptome sequencing in a 6-hydroxydopamine rat model of Parkinson's disease. *Genes & Genetic Systems, 94*(2), 61–69. https://doi.org/10.1266/ggs.18-00036

Liao, Y., Wang, J., Jaehnig, E. J., Shi, Z., & Zhang, B. (2019). WebGestalt 2019: Gene set analysis toolkit with revamped UIs and APIs. *Nucleic Acids Research, 47*(W1), W199–W205. https://doi.org/10.1093/nar/gkz401

Licker, V., Turck, N., Kövari, E., Burkhardt, K., Côte, M., Surini-Demiri, M., Lobrinus, J. A., Sanchez, J.-C., & Burkhard, P. R. (2014). Proteomic analysis of human substantia nigra identifies novel candidates involved in Parkinson's disease pathogenesis. *Proteomics, 14*(6), 784–794. https://doi.org/10.1002/pmic.201300342

Lim, B., Sando, S. B., Grøntvedt, G. R., Bråthen, G., & Diamandis, E. P. (2020). Cerebrospinal fluid neuronal pentraxin receptor as a biomarker of long-term progression of Alzheimer's disease: A 24-month follow-up study. *Neurobiology of Aging, 93*, 97.e1–97.e7. https://doi.org/10.1016/j.neurobiolaging.2020.03.013

Lim, B., Tsolaki, M., Soosaipillai, A., Brown, M., Zilakaki, M., Tagaraki, F., Fotiou, D., Koutsouraki, E., Grosi, E., Prassas, I., & Diamandis, E. P. (2019). Liquid biopsy of cerebrospinal fluid identifies neuronal pentraxin receptor (NPTXR) as a biomarker of progression of Alzheimer's disease. *Clinical Chemistry and Laboratory Medicine (CCLM), 57*(12), 1875–1881. https://doi.org/10.1515/cclm-2019-0428

Ma, Q.-L., Teng, E., Zuo, X., Jones, M., Teter, B., Zhao, E. Y., Zhu, C., Bilousova, T., Gylys, K. H., Apostolova, L. G., LaDu, M. J., Hossain, M. A., Frautschy, S. A., & Cole, G. M. (2018). Neuronal pentraxin 1: A synaptic-derived plasma biomarker in Alzheimer's disease. *Neurobiology of Disease, 114*, 120–128. https://doi.org/10.1016/j.nbd.2018.02.014

Matta, S., Van Kolen, K., da Cunha, R., van den Bogaart, G., Mandemakers, W., Miskiewicz, K., De Bock, P.-J., Morais, V. A., Vilain, S., Haddad, D., Delbroek, L., Swerts, J., Chávez-Gutiérrez, L., Esposito, G., Daneels, G., Karran, E., Holt, M., Gevaert, K., Moechars, D. W., … Verstreken, P. (2012). LRRK2 controls an EndoA phosphorylation cycle in synaptic endocytosis. *Neuron, 75*(6), 1008–1021. https://doi.org/10.1016/j.neuron.2012.08.022

McKetney, J., Runde, R. M., Hebert, A. S., Salamat, S., Roy, S., & Coon, J. J. (2019). Proteomic atlas of the human brain in Alzheimer's disease. *Journal of Proteome Research, 18*(3), 1380–1391. https://doi.org/10.1021/acs.jproteome.9b00004

Moran, L. B., Hickey, L., Michael, G. J., Derkacs, M., Christian, L. M., Kalaitzakis, M. E., Pearce, R. K. B., & Graeber, M. B. (2008). Neuronal pentraxin II is highly upregulated in Parkinson's disease and a novel component of Lewy bodies. *Acta Neuropathologica, 115*(4), 471–478. https://doi.org/10.1007/s00401-007-0309-3

Muraoka, S., Jedrychowski, M. P., Yanamandra, K., Ikezu, S., Gygi, S. P., & Ikezu, T. (2020). Proteomic profiling of extracellular vesicles derived from cerebrospinal fluid of Alzheimer's disease patients: A pilot study. *Cell, 9*(9), 1959. https://doi.org/10.3390/cells9091959

Nägerl, U. V., Eberhorn, N., Cambridge, S. B., & Bonhoeffer, T. (2004). Bidirectional activity-dependent morphological plasticity in hippocampal neurons. *Neuron, 44*(5), 759–767. https://doi.org/10.1016/j.neuron.2004.11.016

Nilsson, J., Constantinescu, J., Nellgård, B., Jakobsson, P., Brum, W. S., Gobom, J., Forsgren, L., Dalla, K., Constantinescu, R., Zetterberg, H., Hansson, O., Blennow, K., Bäckström, D., & Brinkmalm, A. (2023). Cerebrospinal fluid biomarkers of synaptic dysfunction are altered in Parkinson's disease and related disorders. *Movement Disorders, 38*(2), 267–277. https://doi.org/10.1002/mds.29287

Ping, L., Duong, D. M., Yin, L., Gearing, M., Lah, J. J., Levey, A. I., & Seyfried, N. T. (2018). Global quantitative analysis of the human brain proteome in Alzheimer's and Parkinson's disease. *Scientific Data, 5*(1), 180036. https://doi.org/10.1038/sdata.2018.36

Plotegher, N., Kumar, D., Tessari, I., Brucale, M., Munari, F., Tosatto, L., Belluzzi, E., Greggio, E., Bisaglia, M., Capaldi, S., Aioanei, D., Mammi, S., Monaco, H. L., Samo, B., & Bubacco, L. (2014). The chaperone-like protein 14-3-3η interacts with human α-synuclein aggregation intermediates rerouting the amyloidogenic pathway and reducing α-synuclein cellular toxicity. *Human Molecular Genetics, 23*(21), 5615–5629. https://doi.org/10.1093/hmg/ddu275

Riekkinen, P., Kejonen, K., Laakso, M. P., Soininen, H., Partanen, K., & Riekkinen, M. (1998). Hippocampal atrophy is related to impaired memory, but not frontal functions in non-demented Parkinson's disease patients. *Neuroreport, 9*(7), 1507–1511. https://doi.org/10.1097/00001756-199805110-00048

Saal, K.-A., Galter, D., Roeber, S., Bähr, M., Tönges, L., & Lingor, P. (2017). Altered expression of growth associated Protein-43 and rho kinase in human patients with Parkinson's disease. *Brain Pathology (Zurich, Switzerland), 27*(1), 13–25. https://doi.org/10.1111/bpa.12346

Schirinzi, T., Madeo, G., Martella, G., Maltese, M., Picconi, B., Calabresi, P., & Pisani, A. (2016). Early synaptic dysfunction in Parkinson's disease: Insights from animal models: Early synaptic dysfunction in PD. *Movement Disorders, 31*(6), 802–813. https://doi.org/10.1002/mds.26620

Schlimgen, A. K., Helms, J. A., Vogel, H., & Perin, M. S. (1995). Neuronal pentraxin, a secreted protein with homology to acute phase proteins of the immune system. *Neuron, 14*(3), 519–526. https://doi.org/10.1016/0896-6273(95)90308-9

Seyfried, N. T., Dammer, E. B., Swarup, V., Nandakumar, D., Duong, D. M., Yin, L., Deng, Q., Nguyen, T., Hales, C. M., Wingo, T., Glass, J., Gearing, M., Thambisetty, M., Troncoso, J. C., Geschwind, D. H., Lah, J. J., & Levey, A. I. (2017). A multi-network approach identifies protein-specific Co-expression in asymptomatic and symptomatic Alzheimer nons disease. *Cell Systems*, *4*(1), 60–72.e4. https://doi.org/10.1016/j.cels.2016.11.006

Shi, M., Jin, J., Wang, Y., Beyer, R. P., Kitsou, E., Albin, R. L., Gearing, M., Pan, C., & Zhang, J. (2008). Mortalin: A protein associated with progression of Parkinson disease? *Journal of Neuropathology and Experimental Neurology*, *67*(2), 117–124. https://doi.org/10.1097/nen.0b013e318163354a

Sia, G.-M., Béïque, J.-C., Rumbaugh, G., Cho, R., Worley, P. F., & Huganir, R. L. (2007). Interaction of the N-terminal domain of the AMPA receptor GluR4 subunit with the neuronal pentraxin NP1 mediates GluR4 synaptic recruitment. *Neuron*, *55*(1), 87–102. https://doi.org/10.1016/j.neuron.2007.06.020

Silbern, I., Fang, P., Ji, Y., Christof, L., Urlaub, H., & Pan, K.-T. (2021). Relative quantification of phosphorylated and glycosylated peptides from the same sample using isobaric chemical labelling with a two-step enrichment strategy. *Methods in Molecular Biology (Clifton, N.J.)*, *2228*, 185–203. https://doi.org/10.1007/978-1-0716-1024-4_14

Smyth, G. K., Ritchie, M., Thorne, N., & Wettenhall, J. (2005). LIMMA: Linear models for microarray data. In *Bioinformatics and computational biology solutions using R and Bioconductor* (pp. 397–420). New York: Springer. https://doi.org/10.1007/0-387-29362-0_23

Szklarczyk, D., Gable, A. L., Lyon, D., Junge, A., Wyder, S., Huerta-Cepas, J., Simonovic, M., Doncheva, N. T., Morris, J. H., Bork, P., Jensen, L. J., & von Mering, C. (2019). STRING v11: Protein–protein association networks with increased coverage, supporting functional discovery in genome-wide experimental datasets. *Nucleic Acids Research*, *47*(D1), D607–D613. https://doi.org/10.1093/nar/gky1131

Tyanova, S., Temu, T., & Cox, J. (2016). The MaxQuant computational platform for mass spectrometry-based shotgun proteomics. *Nature Protocols*, *11*(12), 2301–2319. https://doi.org/10.1038/nprot.2016.136

Uhlén, M., Fagerberg, L., Hallström, B. M., Lindskog, C., Oksvold, P., Mardinoglu, A., Sivertsson, Å., Kampf, C., Sjöstedt, E., Asplund, A., Olsson, I., Edlund, K., Lundberg, E., Navani, S., Szigyarto, C. A.-K., Odeberg, J., Djureinovic, D., Takanen, J. O., Hober, S., … Pontén, F. (2015). Tissue-based map of the human proteome. *Science*, *347*(6220), 1260419. https://doi.org/10.1126/science.1260419

van der Ende, E. L., Meeter, L. H., Stingl, C., van Rooij, J. G. J., Stoop, M. P., Nijholt, D. A. T., Sanchez-Valle, R., Graff, C., Öijerstedt, L., Grossman, M., McMillan, C., Pijnenburg, Y. A. L., Laforce, R., Binetti, G., Benussi, L., Ghidoni, R., Luider, T. M., Seelaar, H., & van Swieten, J. C. (2019). Novel CSF biomarkers in genetic frontotemporal dementia identified by proteomics. *Annals of Clinical and Translational Neurology*, *6*(4), 698–707. https://doi.org/10.1002/acn3.745

van der Ende, E. L., Xiao, M., Xu, D., Poos, J. M., Panman, J. L., Jiskoot, L. C., Meeter, L. H., Dopper, E. G., Papma, J. M., Heller, C., Convery, R., Moore, K., Bocchetta, M., Neason, M., Peakman, G., Cash, D. M., Teunissen, C. E., Graff, C., Synofzik, M., … van Swieten, J. C. (2020). Neuronal pentraxin 2: A synapse-derived CSF biomarker in genetic frontotemporal dementia. *Journal of Neurology, Neurosurgery & Psychiatry*, *91*(6), 612–621. https://doi.org/10.1136/jnnp-2019-322493

Wang, Y., Yang, F., Gritsenko, M. A., Wang, Y., Clauss, T., Liu, T., Shen, Y., Monroe, M. E., Lopez-Ferrer, D., Reno, T., Moore, R. J., Klemke, R. L., Camp, D. G., & Smith, R. D. (2011). Reversed-phase chromatography with multiple fraction concatenation strategy for proteome profiling of human MCF10A cells. *Proteomics*, *11*(10), 2019–2026. https://doi.org/10.1002/pmic.201000722

Xu, D., Hopf, C., Reddy, R., Cho, R. W., Guo, L., Lanahan, A., Petralia, R. S., Wenthold, R. J., O'Brien, R. J., & Worley, P. (2003). Narp and NP1 form heterocomplexes that function in developmental and activity-dependent synaptic plasticity. *Neuron*, *39*(3), 513–528. https://doi.org/10.1016/S0896-6273(03)00463-X

Yuste, R., & Bonhoeffer, T. (2001). Morphological changes in dendritic spines associated with long-term synaptic plasticity. *Annual Review of Neuroscience*, *24*, 1071–1089. https://doi.org/10.1146/annurev.neuro.24.1.1071

Yuzaki, M. (2018). Two classes of secreted synaptic organizers in the central nervous system. *Annual Review of Physiology*, *80*, 243–262. https://doi.org/10.1146/annurev-physiol-021317-121322

SUPPORTING INFORMATION

Additional supporting information can be found online in the Supporting Information section at the end of this article.